A Microfluidic Device for Whole-Animal Drug Screening Using Electrophysiological Measures in the Nematode C. Elegans

RSC Publishing Lab on a Chip

A microfluidic device for whole-animal drug screening using electrophysiological measures in the nematode C. elegans

Journal:	*Lab on a Chip*
Manuscript ID:	Draft
Article Type:	Paper
Date Submitted by the Author:	n/a
Complete List of Authors:	Lockery, Shawn; University of Oregon, Department of Biology

Cite this: DOI: 10.1039/c0xx00000x

www.rsc.org/xxxxxx

PAPER

A microfluidic device for whole-animal drug screening using electrophysiological measures in the nematode *C. elegans*

Shawn R. Lockery*[a], S. Elizabeth Hulme[b], William M. Roberts[a], Kristin J. Robinson[a], Anna Laromaine[b], Theodore H. Lindsay[a], George M. Whitesides[b], and Janis C. Weeks[a]

Received (in XXX, XXX) Xth XXXXXXXXX 20XX, Accepted Xth XXXXXXXXX 20XX
DOI: 10.1039/b000000x

[a] *Institute of Neuroscience, 1254 University of Oregon, Eugene OR 97403-1254 USA. Fax: 541-346-4548; Tel: 541-346-4590; E-mail: shawn@uoregon.edu*

[b] *Department of Chemistry and Chemical Biology, Harvard University, 12 Oxford St., Cambridge MA 02138 USA.*

† Electronic Supplementary Information (ESI) available: [details of any supplementary information available should be included here]. See DOI: 10.1039/b000000x/

Cite this: DOI: 10.1039/c0xx00000x

www.rsc.org/xxxxxx

PAPER

This paper describes the fabrication and use of a microfluidic device for performing whole-animal chemical screens using non-invasive electrophysiological readouts of neuromuscular function in the nematode worm, *C. elegans*. The device consists of an array of microchannels to which electrodes are attached to form recording modules capable of detecting the electrical activity of the pharynx, a heart-like neuromuscular organ involved in feeding. The array is coupled to a tree-like arrangement of distribution channels that automatically delivers one nematode to each recording module. The same channels are then used to infuse the recording modules with test solutions while recording the electropharyngeogram (EPG) from each worm with sufficient frequency resolution to detect each pharyngeal contraction. The device accurately reported the acute effects of known anthelmintics (anti-nematode drugs) and also correctly distinguished a specific drug-resistant mutant strain of *C. elegans* from wild type. The approach described here is readily adaptable to parasitic species for the identification of novel anthelmintics. It is also applicable in toxicology and drug discovery programs for human metabolic and degenerative diseases in which *C. elegans* is used as a model.

Introduction

Whole-animal screens in small model organisms are gaining acceptance as a means to augment traditional screens based on cultured cells and single-celled organisms[1]. The trend toward whole animal screening is driven in part by advances in genome sequencing, which have revealed a high degree of genetic and biochemical conservation between humans and small, genetically tractable organisms such as the nematode *Caenhorhabditis elegans*[2], the fruit fly *Drosophila melanogaster*[3-5], and the zebrafish *Danio rerio*[6]. A second factor driving this trend is the integration of systems for computerized detection of chemically induced phenotypes with systems that automatically move and sort test organisms[7-11]. As a result, whole-animal testing can now be done earlier in the drug development pathway than ever before, in some cases as early as the primary screening of compound libraries[1, 9]. This change is significant because compounds in whole-animal screens are tested at the level of functional multicellular units including synapses, muscles, and organs rather than isolated cells. Thus, promising compounds (leads) are more likely to succeed in subsequent phases of drug development.

The ability of an automated screening method to identify leads depends critically upon the objective parameters that form the basis of the screen. Such parameters, called readouts or end-points, have therefore been the targets of considerable ingenuity. Readouts fall into two broad categories: (1) assessment of the quantity or anatomical disposition of a fluorescent marker at the cellular[12-14] or organismal[15, 16] level, and (2) quantification of stereotypic behaviors such as crawling[17, 18], swimming[19, 20], or egg laying[21].

Each type of readout represents a unique compromise between cost and information content. The information content of fluorescent-marker readouts is generally low[12] unless image analysis is used[15, 22], but the latter usually requires using a high numerical aperture objective lens with short working distance and narrow field of view, which makes this method expensive to parallelize for whole-animal screens. Behavioral readouts, by contrast, can be obtained with inexpensive optics and thus are more easily parallelized. However, behavioral readouts typically provide less information about the target of drug action because a given behavioral phenotype can be generated by many different biological mechanisms (*e.g.*, cessation of locomotion can result from mechanisms as divergent as ion-channel blockade and disruption of cellular respiration). This drawback can lead to a high rate of detection of compounds that ultimately prove unsuitable for use as drugs (false-positives). Thus, there is a need for readouts that provide more direct information about the target of drug action, and are practical to parallelize.

Here we present a new whole-animal screening method that uses a non-invasive electrophysiological readout of neuromuscular function. The screen is based on monitoring the activity of the nematode throat (pharynx), a muscular pump that contracts rhythmically to draw liquid nutrients into the digestive tract during feeding. As in the vertebrate heart, rhythmic contractions of the nematode pharynx are generated primarily by the pharyngeal muscles themselves, and each contraction is associated with an action potential, a large voltage transient that can be recorded by electrodes placed on the surface of the body[23]. By analogy to an electrocardiogram, such a recording in nematodes is called an electropharyngeogram (EPG). In addition to registering action potentials in the pharyngeal muscles, the EPG also registers the activity of neurons that regulate the rate of pharyngeal pumping in much the same way as the autonomic nervous system regulates the vertebrate heart. Thus, the EPG can be used to investigate the effects of drugs that act on neurons as well as muscles.

Using soft-lithography, we constructed a device that permits simultaneous recording of EPGs from eight nematodes before, during, and after delivery of a test compound. To validate the utility of the device, we demonstrate here that it rapidly and reliably detects the acute effects of anthelmintics (anti-nematode drugs) and also correctly distinguishes a specific drug-resistant mutant strain of *C. elegans* from wild type. In addition to facilitating the search for new anthelmintics, the device is expected to be useful in two broad areas: toxicology and drug discovery programs, in which *C. elegans* serves as a model for human diseases including a variety of metabolic and degenerative disorders[2].

Methodology

Conventional EPG recording method

In the conventional EPG recording method[23], the worm is immersed in a bath of physiological saline and sucked into a saline-filled glass pipette (Fig. 1). Pharyngeal activity is induced by adding the neuromodulator serotonin to the bath saline, which initiates feeding behavior in *C. elegans*[24]. Because the saline is conductive, electrodes in the bath and the pipette are in electrical contact with the surface of the body. The conventional method is ill-suited to drug screens in two key respects. First, to attain this recording configuration, the operator must capture the worm by manual adjustment of a micromanipulator that holds the pipette

(not shown); this form of capture would be difficulty to automate and parallelize. Second, drugs are delivered via the bath solution, thus requiring macroscopic volumes of drug solutions.

Microfluidic EPG device

To adapt EPG recording approach for drug screening, we constructed a device that automatically loads individual worms into eight recording modules for simultaneous EPG recording from multiple worms (Fig. 2A). The device is fabricated from a single layer of polydimethylsiloxane (PDMS), using standard methods of soft-lithography[25, 26] and bonded to a glass substrate after exposure to an air plasma. The array of recording modules is served by a bifurcating, tree-like arrangement of distribution channels. When a buffer solution containing worms is injected into the inlet port of the device, the solution flows through all open channels, causing animals to segregate passively into separate recording modules until each is blocked by a worm[8].

Within each recording module, the worm is carried by the flowing fluid until it reaches a constriction (henceforth "trap") into which only the worm's head or tail, which are narrower than the rest of the body, can fit. The trapped worm obstructs the worm channel, diverting most of the flow into the side-arm channel. This arrangement allows test solutions injected into the inlet port to continue to flow past the trapped worms while the EPG is recorded. Two waste reservoirs collect perfusate from the worm trap and side-arms, respectively. For long-term experiments (>6 h), the capacity of the waste reservoirs can be increased by inserting tight-fitting glass tubes.

Electrical recordings are made by means of metal electrodes inserted into the worm electrode ports and the joint inlet/reference electrode port (Fig. 2A). Each of the worm electrodes is connected to the positive input of one of a bank of eight differential amplifiers (see Experimental Methods). The common reference electrode is connected to the negative inputs of all amplifier channels. The reference electrode is hollow to permit perfusion of test solutions during EPG recordings.

To optimize electrical recordings and solution delivery, it is important that the head or tail of the worm enters the trap rather than one of the side-arm openings. Three aspects of the design ensure that this happens. First, the dimensions of the side-arm channel openings (10 μm × 20 μm) are small compared to the diameter of the worm (70 – 90 μm). Second, dimensions of channels leading away from the recording module are adjusted such that the calculated hydrodynamic resistance to flow through the side arms to Reservoir 2 is 20 times the resistance to flow through the worm trap to Reservoir 1. Thus, as a worm enters a recording module, ~95% of the flow is toward the worm trap rather than the side arms. Third, the funnel-shaped entrance to the worm trap aligns the worm so that its head or tail is driven into the trap (Fig. 2E). The design of the recording module thus ensures a snug fit of the worm in the trap, creating a sufficiently large electrical resistance (R_{seal}) to record the EPG with a high signal-to-noise ratio (SNR; Fig. 2D), without unduly compromising the flow of test solutions around the worm.

Worms were held in position throughout an experiment by positive pressure exerted by solutions perfused into the device via a syringe pump. Flow rate was adjusted so that approximately one third of the pharynx of a headfirst worm remained in the funnel-shaped region of the worm channel where it was exposed to perfused solutions. During tailfirst recordings, a similar length of the worm's body was lodged in the worm trap, and the head was completely exposed to the solution. The optimum flow rate depended on the relative size of the worm and the worm trap, with the effective range of flow rates for young adult *C. elegans* being approximately 5 to 50 μL/min. Below this range, the SNR was too low (*e.g.*, Fig. 2D); above this range, the worm was often forced through the trap. Under typical recording conditions, median SNR was 100 (n = 7), which was sufficient to observe detailed features of the EPG recordings.

Results and Discussion

Parallel microfluidic electropharyngeograms

The waveforms of EPGs recorded using the microfluidic device were similar to those obtained using conventional EPG recording methods[23, 24, 27-30] (Fig 3A,B). The EPGs recorded from worms oriented tailfirst in the trap were similar to EPGs from headfirst worms except that the polarity was reversed[23]. Referring to the canonical headfirst recording configuration (Fig. 3A, B), the most prominent features were a positive spike (E), caused by the rapid depolarizing phase of the pharyngeal muscle action potential that initiates contraction, and a negative spike (R) caused by the rapid repolarization of the pharyngeal muscle that terminates the contraction[23]. Smaller downward peaks, which have been attributed to activity of neurons that modulate pharyngeal pumping[23], were often visible between E and R transients.

The array of recording modules made it possible to record from eight worms at a time (Fig. 3C), but in some cases not all were usable. Overall, the probability that a recording module yielded a usable EPG recording was 0.75 (N = 348 modules). The most common cause of recording failure was an air bubble between the worm and one of the electrodes. In other cases, a worm failed to pump or there was more than one worm in the module. In standard saline (M9-5HT buffer, see Experimental Methods), pharyngeal pumping and EPG recordings such as those in Fig. 3C typically continued for 6 to 8 hours and, although not investigated systematically, sometimes overnight. Thus, the device is suitable for medium-throughput experiments involving acute or semi-chronic exposure of multiple worms to small volumes of test compounds.

Delivery of test compounds

To demonstrate the ability to record EPGs in the presence of test compounds, we perfused the anthelmintic ivermectin during simultaneous EPG recordings from six worms (Fig. 4A). Ivermectin inhibits pharyngeal muscles and extrapharyngeal neurons by activating a class of glutamate-gated chloride channels located in the plasma membrane[31, 32]. Perfusion of ivermectin blocked pharyngeal activity within 10-15 min[28, 33], regardless of whether the worms were oriented headfirst or tailfirst. Pharyngeal activity was unaffected in worms that underwent a mock solution change (Fig. 4B), indicating that the cessation of activity was specific to the presence of the drug. Pharyngeal activity persisted in ivermectin-resistants mutants in which the three main muscular and neuronal targets of ivermectin are altered[32] (Fig. 4C), indicating that the full effect of ivermectin in the EPG device requires the presence of previously established molecular targets. EPGs recorded in ivermectin also exhibited the expected reduction in the amplitude of the E and R spikes[28, 33] (Fig. 5A). We conclude that test compounds reach the worms and have the expected pharmacological effects, for both headfirst and tailfirst orientation of the worm in the trap.

In addition, we detected two previously unreported effects of ivermectin. First, we observed a reduction in the duration of the action potentials, measured as the interval between pairs of E and R spikes (Fig. 5A; see Fig. 6 below). Second, we observed an increase in the frequency of gaps in the otherwise regular pattern of action potential firing (Fig. 5B). Changes in action potential duration and appearance of gaps have been reported in mutants with loss of function defects in the molecular target of the anthelmintic emodepside[29, 34]. This

suggests that such effects may be common features of certain classes of anthelmintics.

Analysis of action potential waveform

Automated data analysis is an essential component of many practical screening approaches and such analysis methods have recently been introduced for EPG data[29, 34]. In addition to being objective and efficient, automated EPG analysis can measure parameters that provide valuable insights into the mode of action of a given test compound[34]. To demonstrate application of automated methods to EPG recordings obtained in the microfluidic EPG device, we quantified EPG records using three common metrics of pharyngeal activity: (1) peak-to-peak amplitude, defined as the voltage difference between the E and R peaks; (2) instantaneous pumping frequency, defined as the reciprocal of the time between successive E peaks; and (3) action potential duration, defined as the time interval between the E and R peaks in a single pumping event. Ivermectin caused a gradual reduction all three measures (Fig. 6). The plot of instantaneous pumping frequency also revealed the appearance of many low frequency events as the drug began to take effect (Fig. 6B, 20 – 40 min). Inspection of the raw data showed that these events corresponded to the above-mentioned gaps in the regular firing pattern of action potentials (Fig. 5B). Each of the effects shown in Fig. 6 is consistent with the activation of an inhibitory conductance in pharyngeal muscles, and is thus in agreement with the previously established mechanism of ivermectin activity[31] . This finding illustrates the utility of the present method in mode of action studies.

Analysis of EPG amplitude

Automated analysis of EPG data is sensitive to variations in action potential waveform across individual worms, and over time in response to test compounds[29]. This problem arises because extraction of spike frequency and related parameters requires the use of peak detection algorithms which can be sensitive to the shape and amplitude of the underlying events. Although this sensitivity can be mitigated to a large degree by customizing the peak detection algorithm for each worm, doing so on the large data sets generated by parallel EPG recordings may be impractical in some screening applications. Here we show that simply computing the magnitude of the EPG signal can be diagnostic for the effects of drugs and genetic backgrounds (Fig. 7). We computed EPG magnitude by taking the absolute value of the voltage at each time point and smoothing the result (see Experimental Methods). The background noise level, measured when pharyngeal pumping had stopped, was then subtracted, yielding a time series that we refer to as $||EPG||(t)$. This time series compactly represents two of the main features of each EPG recording, changes in the amplitude and frequency of action potentials over time. In Fig. 7A-C, $||EPG||(t)$ is plotted for three individual worms, one from each of the three conditions shown in Fig. 4. Group data were obtained by normalizing individual $||EPG||(t)$ data to a value of 1 immediately prior to the solution change, then averaging across worms.

Fig. 7D shows group data for the three conditions studied in the experiment of Fig. 4. All three curves were widely separated relative to the standard error of the mean, showing that the effects of ivermectin on wild type and ivermectin-resistant mutants were quantitatively different, even with small sample sizes (≤ 6 animals per group; see figure legend for statistics). The amplitude of the EPG in control animals increased over time. Although further experiments are required, we speculate that worms were gradually pushed further into the traps as time progressed, increasing R_{seal}.

Fig. 7E shows a similar experiment in which the anthelmintic levamisole was used instead of ivermectin. As expected[35], levamisole also caused rapid and complete reduction of $||EPG||(t)$. Significantly, the ion channels that levamisole targets are present on body wall muscles[36] and are not required for normal pharyngeal pumping[37]. Thus, the microfluidic EPG device can detect anthelmintic drug activity even when a drug may be acting primarily at extrapharyngeal sites. We also found that, in contrast to the effects of ivermectin, the effects of levamisole on wild type and imvermectin-resistant mutants were indistinguishable (see figure legend for statistics). This finding indicates that the EPG device could be used to characterize the effects of drugs on a wide range of resistance mutants or other genetic backgrounds that could be useful in assigning test compounds to existing (or novel) modes of action.

Conclusions

The device presented here permits simultaneous, individualized recordings of electrical activity from up to eight nematodes during the application of drugs and other test compounds. The number of simultaneous recordings could be increased by recording from many devices in parallel, by increasing the number of recording modules per device, or both. The practical limit to the throughput of the microfluidic EPG approach is not yet known, but distribution channels for positioning more than 100 nematodes at a time have been demonstrated[8].

Modifications to the current design using existing technology could enhance its utility. For large numbers of simultaneous recordings it would be advantageous to add microfabricated electrodes[38] to facilitate automated connection to the recording equipment. The quantity of test compound required could be reduced by incorporating on-chip drug reservoirs. Importantly, the dimensions of distribution channels and recording modules could be adjusted to accommodate other species of nematodes. This modification would allow for direct, medium-throughput assessment of compounds to treat nematodes in a wide range of hosts from plant to humans[39].

Experimental Methods

Nematodes

C. elegans strains were grown on Nematode Growth Medium (NGM) agar plates seeded with the OP_{50} strain of E. coli. All strains were obtained from the Caenorhabditis Genetics Center (CGC; Minneapolis, MN). Wild-type worms were Bristol N2 and Ivermectin (IVM) resistant mutants were DA1316 avr-14 (ad1302); avr-15(ad1051); glc-1(pk54). Adult hermaphrodites were used for all experiments with the exception of SNR measurements, which also included some L4 animals. Animals were age-synchronized by one of two methods: (1) L4s were transferred to a seeded NGM plate and left overnight at room temperature to develop into adults; or (2) gravid adults were placed on seeded NGM plates to lay eggs for ~6 hr and then removed, with the plates maintained at room temperature until the adults matured.

Device Fabrication

We fabricated devices using standard soft lithographic methods[25, 26]f. Briefly, a silicon wafer master for the device was created by exposing a 55 μm layer of SU-8 2050 resist (Microchem, Newton, MA) through a transparency mask and dissolving away unexposed material. Masters were replica-molded in PDMS, Dow Corning Sylgard 184, Corning, NY) and treated with chlorotrimethylsilane (Aldrich, St. Louis, MO) to prevent

adhesion of PDMS to the master. Holes for ports, inlets, and fluid reservoirs were formed using biopsy punches of the appropriate diameter (ports and inlets, 1.5 mm; reservoirs, 5 mm). PDMS castings were bonded to glass substrates after 30 sec exposure to an oxidizing air plasma. After bonding, the capacity of each fluid reservoir was increased by inserting a 1.5 cm length of 5 mm glass tubing.

Solutions

All experiments utilized M9 buffer[40] containing KH_2PO_4, $NaHPO_4$, NaCl and $MgSO_4$, to which serotonin (5HT) was added to stimulate pharyngeal pumping[23]. Stocks of serotonin creatine sulfate monohydrate (Sigma H7752; St. Louis, MO) were prepared in M9 buffer at 40 mM and held in small aliquots at -20°C until use. Each day of an experiment, a fresh aliquot was thawed and diluted to 10 mM 5HT in M9 buffer. This "M9-5HT" buffer was the control medium to which drugs or other compounds were added. Stock solutions of ivermectin (10 mM; Sigma 8898) were made up in 100% dimethyl sulfoxide (DMSO; Fisher D-136; Fair Lawn, NJ) and held at -20°C for no longer than 2 wk. Control experiments (not shown) indicated that DMSO at the final concentrations used for perfusions (≤ 0.1%) did not adversely affect EPG activity. Stock solutions of levamisole hydrochloride (100 mM; Sigma 31742) were made up in sterile dH_20 and maintained at 4°C. On the day of an experiment, IVM or LEV stocks were diluted to the final concentration in M9-5HT buffer that contained 0.005% Fast Green (Fisher F-99) as a visual indicator of drug flow within the device (see below); the dye-containing buffer was filtered (PALL Life Sciences 25mm Acrodisc syringe filter with 0.2 µm HT Tuffryn Membrane; Port Washington, NY) before adding test compounds.

Loading worms into the device

Young adult worms were transferred from growth plates into a glass well containing M9-5HT buffer and left to acclimate for 10 min. While viewed under transillumination on a Stemi SV6 binocular stereomicroscope (Carl Zeiss Inc., Thornwood, NY), 8 worms were picked using a loop tool and placed into the inlet port of the device, which had been preloaded with M9-5HT buffer. A 3 cc syringe filled with M9-5HT buffer connected to a length of 1.5 mm polyethylene tubing was then inserted into the inlet port and gentle pressure was applied to propel worms into the eight individual worm channels in the device. The tubing connected to the inlet port was then removed and the loaded device was moved to the EPG recording apparatus.

Electrophysiological recordings

EPGs were recorded by a pair of 4-channel AC differential amplifiers (A-M Systems model 1700, Carlsborg, WA) connected to electrodes inserted into the device. Electrodes were made from 0.5 inch long passivated 17 gauge stainless steel tubes (0.058 inch OD, 0.0475 inch ID, New England Small Tube, Litchfield, NH).

Recordings were made at voltage gains of 1,000× or 10,000× and filtered with a low-pass cutoff of 1.0 Hz and a high-pass cutoff of 5 kHz. Signals were further conditioned by a 60 Hz notch filter. Signals were displayed on a pair of four channel oscilloscopes (TDS 2024B, Tektronix, Beaverton, OR) at a sweep speed sufficient to resolve the components of individual pharyngeal action potentials. Signals were recorded for later analysis using a data acquisition system (Micro1401-3, Cambridge Electronic Design (CED), Cambridge, UK) connected to a computer running Spike2 software (version 7.06a, CED). Data were sampled at 5 or 10 kHz per channel. An additional channel was used as a keystroke-controlled event marker (e.g., time of drug delivery). Data were typically acquired continuously in Spike 2, beginning when electrodes were inserted into the device and continuing until an experiment was terminated (generally 1-2 h after drug addition). For long recording sessions (e.g., overnight), Spike2 was set to acquire short data segments at regular intervals (e.g., 5 min of recording every 20 min).

Solution delivery

Solutions were delivered to EPG devices via a syringe pump (Harvard Apparatus PHD 2000; Holliston, MA) driving a pair of 3 cc syringes. One syringe was filled with M9-5HT buffer while the other contained M9-5HT buffer with 0.005% Fast Green to which was added nothing (for control experiments), drug, drug plus vehicle or vehicle alone. Each syringe was fitted with a 25 gauge stub needle that led via a 30 cm length of fine polyethylene tubing (BPE-T25, Instech Solomon, Plymouth Meeting, PA, USA) to the hollow metal reference electrode (see above). Following pilot experiments investigating the relationship between perfusion rate and EPG signal-to-noise (SNR) ratio (see Results), a perfusion rate of 6 µl/min was used. Solution changes were effected by removing the reference electrode connected to the first syringe from the fluid inlet port of the device and inserting the reference electrode connected to the second syringe. This procedure eliminated potential cross-contamination between solutions. The perfusion line from the syringe not in use was led to a waste receptacle. The latency between insertion of the electrode and arrival of the new solution at the worm's location, as visualized by dye movement, was approximately 60 sec. The electrical artifact from switching reference electrodes was subsequently blanked from recordings shown in Figures.

Calculation of ||EPG||(*t*)

A simple analysis, which did not involve identifying the occurrences of individual pharyngeal contractions, was used to quantify the decline in the EPG amplitude with time after drug application. For this analysis EPG(*t*) was band-pass filtered in Spike2 (2 – 200 Hz, 2-pole Bessel filters), down-sampled at 500 Hz, full-wave rectified, and smoothed (exponential filter, time constant = 60 s), to yield ||EPG||(*t*), a measure that is proportional to both the frequency and strength of pharyngeal contractions. In experiments during which pharyngeal pumping ceased completely for a period of time, the baseline noise was removed by subtracting the minimum value of ||EPG||(*t*) during the experiment. The mean baseline noise determined in this way was 3.7 ± 0.5 µV (mean ± S.D., n = 24 worms). In experiments in which pharyngeal pumping never ceased, the baseline noise was assumed to be 3.7 µV.

Analysis of EPG features

To analyze the effects of test solutions on frequency, strength, and other aspects of pharyngeal pumping separately, we identified the onset of pharyngeal muscle contraction and relaxation during each pump cycle (Fig. 3). For this analysis, we inverted the sign of EPGs obtained from worms that were oriented tail-first in the recording chamber. EPGs were high-pass filtered to aid in separating the E and R peaks from the slower components of the EPG waveform and from low-frequency noise before locating all positive and negative peaks that exceeded threshold values.. Event times were then measured as the times of the corresponding peaks in the unfiltered EPG. Positive and negative thresholds and high-pass filter frequencies were set by the user for each worm. Valid EPG events were defined as a positive peak followed by a negative peak with no intervening positive or

negative peaks. For each valid EPG event we recorded the time interval between the positive and negative peaks, which corresponds to the duration of the contraction of the pharyngeal muscles[23], and the voltage difference between the positive and negative peaks (peak-to-peak amplitude), which reflects the size and speed of the muscle depolarization and repolarization. The peak-to-peak amplitude is also sensitive to changes in R_{seal}. We measured pump frequency as the reciprocal of the time interval between the positive peaks of successive valid EPG events.

Calculation of SNR

Signal to noise ratio was defined as $SNR = (\sigma_T^2 - \sigma_N^2)/\sigma_N^2$, where σ_T^2 was the total variance of the EPG recording during vigorous pumping (~5 Hz) and σ_N^2 was the variance during periods in which pumping spontaneously ceased.

Measurement of R_{seal}

We determined typical values for (R_{seal}) by applying a voltage step between the positive electrode for a recording module and the common reference electrode, and measuring the resulting electric current. Because of the small cross-sectional area of the channels in the microfluidic device, the electrical resistance was relatively high even when the recording channel was unoccupied by a worm (~5 MΩ). This resistance increased to ~6 MΩ with a worm loosely positioned in the channel, and typically increased by ~200 kΩ with the worm snugly in the trap, from which we estimate that Rseal ≈ 200 kΩ, similar to seal resistances obtained in "loose-seal" patch recordings[41]. Given the relatively small value of R_{seal} compared to the resistance of the unoccupied channel, is perhaps surprising that the SNR increased 9-fold when the worm's head entered the trap, but this result is consistent with the conclusion that EPG is primarily the result of current flowing out of the mouth[23], which becomes electrically isolated from the rest of the body when the head is held snugly in the trap. It is unclear why the SNR also increased greatly when the tail of the worm entered the trap, but we speculate that the major return current pathway for the EPG may be through the worm's anus.

Acknowledgements

Support: SRL, John Simon Guggenheim Foundation; NIH Challenge Grant RC1AI087059; and University of Oregon Technology Entrepreneurship Program. SEH, American Society for Engineering Education National Defense Science and Engineering Graduate Fellowship. GMW, Bill and Melinda Gates Foundation award 51308. Consultation: L. Avery, J. Dent, T. Geary, X. Liu, A. Sluder, J. C. W. Roberts.

Cite this: DOI: 10.1039/c0xx00000x

www.rsc.org/xxxxxx

PAPER

References

1. J. Giacomotto and L. Segalat, *Br J Pharmacol*, 2010, **160**, 204-216.
2. T. Kaletta and M. O. Hengartner, *Nat Rev Drug Discov*, 2006, **5**, 387-398.
3. E. Bier, *Nat Rev Genet*, 2005, **6**, 9-23.
4. R. Drysdale, *Methods Mol Biol*, 2008, **420**, 45-59.
5. G. M. Rubin and E. B. Lewis, *Science*, 2000, **287**, 2216-2218.
6. G. Kari, U. Rodeck and A. P. Dicker, *Clin Pharmacol Ther*, 2007, **82**, 70-80.
7. S. E. Hulme, S. S. Shevkoplyas, A. P. McGuigan, J. Apfeld, W. Fontana and G. M. Whitesides, *Lab Chip*, **10**, 589-597.
8. S. E. Hulme, S. S. Shevkoplyas, J. Apfeld, W. Fontana and G. M. Whitesides, *Lab Chip*, 2007, **7**, 1515-1523.
9. M. F. Yanik, C. B. Rohde and C. Pardo-Martin, *Annu Rev Biomed Eng*, 2011, **13**, 185-217.
10. D. Wlodkowic, K. Khoshmanesh, J. Akagi, D. E. Williams, J. M. Cooper and X. X. Xxxx, *Cytometry A*, 2011, **79**, 799-813.
11. R. T. Peterson, R. Nass, W. A. Boyd, J. H. Freedman, K. Dong and T. Narahashi, *Neurotoxicology*, 2008, **29**, 546-555.
12. R. Pulak, in *Methods in Molecular Biology*, ed. K. Strange, 2006, vol. 351, pp. 275-286.
13. W. A. Boyd, M. V. Smith, G. E. Kissling and J. H. Freedman, *Neurotoxicol Teratol*, **32**, 68-73.
14. S. J. Gosai, J. H. Kwak, C. J. Luke, O. S. Long, D. E. King, K. J. Kovatch, P. A. Johnston, T. Y. Shun, J. S. Lazo, D. H. Perlmutter, G. A. Silverman and S. C. Pak, *PloS ONE*, **5**, e15460.
15. C. B. Rohde, F. Zeng, R. Gonzalez-Rubio, M. Angel and M. F. Yanik, *Proc Natl Acad Sci U S A*, 2007, **104**, 13891-13895.
16. M. M. Crane, K. Chung and H. Lu, *Lab Chip*, 2009, **9**, 38-40.
17. S. D. Buckingham and D. B. Sattelle, *Invert Neurosci*, 2008, **8**, 121-131.
18. J. A. Carr, A. Parashar, R. Gibson, A. P. Robertson, R. J. Martin and S. Pandey, *Lab Chip*, **11**, 2385-2396.
19. K. Chung, M. Zhan, J. Srinivasan, P. W. Sternberg, E. Gong, F. C. Schroeder and H. Lu, *Lab Chip*, **11**, 3689-3697.
20. G. J. Lieschke and P. D. Currie, *Nat Rev Genet*, 2007, **8**, 353-367.
21. B. R. Ellerbrock, E. M. Coscarelli, M. E. Gurney and T. G. Geary, *J Biomol Screen*, 2004, **9**, 147-152.
22. K. Chung, M. M. Crane and H. Lu, *Nature methods*, 2008, **5**, 637-643.
23. D. M. Raizen and L. Avery, *Neuron*, 1994, **12**, 483-495.
24. R. J. Hobson, V. M. Hapiak, H. Xiao, K. L. Buehrer, P. R. Komuniecki and R. W. Komuniecki, *Genetics*, 2006, **172**, 159-169.
25. Y. Xia, E. Kim, X. M. Zhao, J. A. Rogers, M. Prentiss and G. M. Whitesides, *Science*, 1996, **273**, 347-349.
26. Y. Xia and G. M. Whitesides, *Annual Review of Materials Science*, 1998, **28**, 153-185.
27. J. A. Dent, M. W. Davis and L. Avery, *EMBO J*, 1997, **16**, 5867-5879.
28. J. C. Sheriff, A. C. Kotze, N. C. Sangster and R. J. Martin, *Parasitology*, 2002, **125**, 477-484.
29. J. Dillon, I. Andrianakis, K. Bull, S. Glautier, V. O'Connor, L. Holden-Dye and C. James, *PloS ONE*, 2009, **4**, e8482.
30. M. W. Davis, D. Somerville, R. Y. Lee, S. Lockery, L. Avery and D. M. Fambrough, *J Neurosci*, 1995, **15**, 8408-8418.
31. J. A. Dent, M. M. Smith, D. K. Vassilatis and L. Avery, *Proc Natl Acad Sci U S A*, 2000, **97**, 2674-2679.
32. A. J. Wolstenholme and A. T. Rogers, *Parasitology*, 2005, **131 Suppl**, S85-95.
33. D. J. Pemberton, C. J. Franks, R. J. Walker and L. Holden-Dye, *Mol Pharmacol*, 2001, **59**, 1037-1043.
34. A. Crisford, C. Murray, V. O'Connor, R. J. Edwards, N. Kruger, C. Welz, G. von Samson-Himmelstjerna, A. Harder, R. J. Walker and L. Holden-Dye, *Mol Pharmacol*, **79**, 1031-1043.
35. P. R. Towers, B. Edwards, J. E. Richmond and D. B. Sattelle, *J Neurochem*, 2005, **93**, 1-9.
36. J. T. Fleming, M. D. Squire, T. M. Barnes, C. Tornoe, K. Matsuda, J. Ahnn, A. Fire, J. E. Sulston, E. A. Barnard, D. B. Sattelle and J. A. Lewis, *J Neurosci*, 1997, **17**, 5843-5857.
37. L. Avery, *J Exp Biol*, 1993, **175**, 283-297.
38. A. Pavesi, F. Piraino, G. B. Fiore, K. M. Farino, M. Moretti and M. Rasponi, *Lab Chip*, **11**, 1593-1595.
39. S. E. Hulme and G. M. Whitesides, *Angew Chem Int Ed Engl*, **50**, 4774-4807.
40. J. E. Sulston and J. A. Hodgkin, in *The nematode Caenorhabditis elegans*, eds. W. B. Wood and T. C. o. C. e. Researchers, Cold Spring Harbor Laboratory Press, Plainview, NY, 1988, pp. 587-606.
41. W. M. Roberts, *The Journal of physiology*, 1987, **388**, 213-232.

Legends

Figure 1. Diagram of the conventional method of recording an electropharyngeogram (EPG). A worm is submerged in a bath of physiological saline and the anterior end is sucked into a tight-fitting, saline-filled glass pipette. The tight apposition between the worm's body and the mouth of the pipette generates an electrical resistance (R_{seal}) between the lumen of the pipette and the bath. As a result of this resistance, electrical currents generated by pharyngeal activity can be detected directly, or by means of the voltage difference (V) that is generated between the pipette and the bath[23]. The microfluidic EPG device described in Fig. 2 replicates the recording topology illustrated here.

Figure 2. Design of the microfluidic EPG device. A. Top view of the overall device. Arrows indicate the direction of fluid flow. B. Top view of a single recording module. The inset shows the funnel-shaped entrance to the worm trap and position of the head of the worm in the trap under headfirst recording conditions. Color indicates feature height (black, 50 μm; gray, 10 μm). C. Three dimensional rendering of the recording module. D,E. Enhancement of signal-to-noise ratio (SNR) by positioning worm snugly in the worm trap. D. Micrograph of the recording module and the associated EPG recording with the syringe pump turned off. E. Micrograph of the recording module and the associated EPG recording with the syringe pump turned on, forcing the worm's head into the trap. Anterior is to the right and the recordings are shown on the same vertical scale in both panels. In D and E, arrowheads indicate the posterior margin of the pharynx.

Figure 3. EPG recordings obtained by the conventional method and the microfluidic device. A. Pharyngeal action potential recorded using the conventional method shown in Fig. 1 (reproduced from Fig. 2A of reference[23]). E and R indicate the large positive (Excitatory) and negative (Relaxation) spikes, respectively, at the beginning and end of the action potential. The worm was oriented headfirst in the pipette. B. Pharyngeal action potential recorded using the microfluidic EPG device. Symbols and worm orientation are as in A. The scale bar in B refers to A and B. C. Simultaneous recordings from 8 worms in a single microfluidic EPG device. All worms except 2 and 8 were oriented headfirst in the worm trap. Vertical scales (voltage) were adjusted to produce similar signal amplitudes in all traces. The data on the left are duplicated at right on a compressed time axis, to illustrate how recordings are displayed in Figs. 4 and 7.

Figure 4. Ivermectin effects on wild type and ivermectin-resistant worms. Each panel shows simultaneous EPG recordings from a single microfluidic EPG device, each containing both headfirst and tailfirst worms. Dashed lines replace data segments obscured by electrical artifacts during the solution change. Vertical scales (voltage) were adjusted to produce similar signal amplitudes in all traces; the horizontal scale bar (time) in C applies to all panels. In all experiments, worms were first perfused with control solution (M9-5HT buffer for >30 min before switching to drug or control solution containing 0.005% Fast Green as a visual marker. A. 3 μM ivermectin rapidly blocked EPG activity in wild type worms. B. EPG activity continued robustly during mock solution change in wild type worms. C. 3 μM ivermectin only partially inhibited EPG activity in ivermectin-resistant mutant worms *(DA1316 avr-14(ad1302); avr-15(ad1051); glc-1(pk54))* compared to wild type worms (compare with A).

Figure 5. Changes in EPG waveform and frequency during ivermectin treatment. A and B each show representative recordings from a single wild type worm at the times indicated at left, relative to the switch from control solution to ivermectin (designated 0 min). Vertical gain (voltage) is the same for all traces within a panel. A. Changes in EPG waveform. This worm was headfirst in the channel and EPG traces are aligned (vertical dashed line) by the onset of a positive E spike, except for the bottom trace which occurred after EPG activity ended. The ivermectin concentration was 10 μM. Filled bars show E-to-R duration for each action potential waveform; filled circles indicate action potentials waveforms with an E but no R spike; open bars indicate voltage excursion of EPG waveforms in in the adjoining trace. The EPG Action potentials waveform became progressively smaller and briefer, pumping frequency decreased and the R spike of the waveform was lost. B. Changes in action potential timing. In control solution, pumping was regular in frequency and large in amplitude, with approximately symmetric E and R spikes phases (this worm was tailfirst in the channel so E spikes are downward in the figure). In response to 0.1 μM ivermectin, the rhythm began to exhibit gaps that lengthened progressively over time, resulting in intermittent bouts of pumping. Pumping frequency within each bout decreased moderately over time, as did spike amplitude. Eventually only isolated pumps dominated by the E spike remained.

Figure 6. Effect of ivermectin on peak-to-peak EPG amplitude (A1), pump frequency (B1) and duration of pharyngeal action potentials (C1) for one representative wild type worm. The worm was first perfused with control solution (M9-5HT buffer for >30 min before switching to 0.1 μM ivermectin containing 0.005% Fast Green as a visual marker. The drug reached the worm at t = 0. Each dot in A1, B1, C1 corresponds to a single pump as defined by the detection algorithm (see Experimental Methods). The events were divided into four time regions (−10 to −0.5 min, black; 0.3 to 20 min, magenta; 20 to 35 min, green; 35 to 50 min, blue). The corresponding probability distributions (PDFs) for the data points are shown in A2, B2, C2 using the same color scheme. The peak-to-peak amplitude began to decline toward zero ~20 min after drug application, until pumps became undetectable after 50 min. The modal pumping frequency remained nearly constant at ~5.2 Hz (B, black and magenta) until ~20 min after drug application, then began to decline. At later times, long inter-event intervals became increasingly frequent, causing the modal pump frequency to switch to a much lower frequency (0.6 Hz) after 40 min (blue dots in B1 and blue trace in B2). The duration of pharyngeal action potentials contractions (C) began to decline ~15 min after drug application from the initial modal duration of 104 ms (black and magenta) to 52 ms (green and blue). Neither the frequency nor duration of action potentials was noticeably altered during transient epochs of increased amplitude (x's in A1), which we speculate were probably caused by movement of the worm within the worm recording module.

Figure 7. Effects of ivermectin and levamisole on the EPG and its magnitude $||EPG||(t)$ in wild type and ivermectin-resistant mutants. Dashed lines replace data segments obscured by electrical artifacts during the solution change. A-C show representative EPG data from three individual worms. D and E show $||EPG||(t)$, normalized to the value immediately before the solution change, and averaged across 5 or 6 worms per condition; grey regions show ±1 SD. In all experiments, worms were first perfused with control solution (M9-5HT buffer) for >30 min before switching at t = 0 to a test solution that contained 3 μM ivermectin (A,C and colored traces in D), 10 mM levamisole (colored traces in E), or control solution (B, black traces in D and E), with 0.005% Fast Green as a visual marker in each case. Ivermectin-resistant worms *(DA1316 avr-14(ad1302); avr-15*

(ad1051); glc-1(pk54)) were used for panel C and for the red traces in D and E; all other worms were wild type. By $t = 6$ min after exposure to ivermectin, the mean normalized ||EPG||(t) was significantly reduced in wild type worms (D, blue) compared to controls (D, black; $p < 0.03$; two-tailed t-test), but not in ivermectin-resistant mutants (D, red; $p > 0.5$). After 20 min exposure to ivermectin, ||EPG||(t) was significantly reduced in wild type and mutants compared to controls ($p < 0.02$), but remained significantly higher in mutants than in wild type worms for the duration of these ivermectin experiments ($t = 60$ min; $p < 0.02$). As expected, levamisole caused rapid inhibition of pharyngeal pumping in both wild type (E, blue) and ivermectin-resistant (E, red) worms compared to controls (E, black; $p < 0.0001$ at $t = 6$ min, for both comparisons).

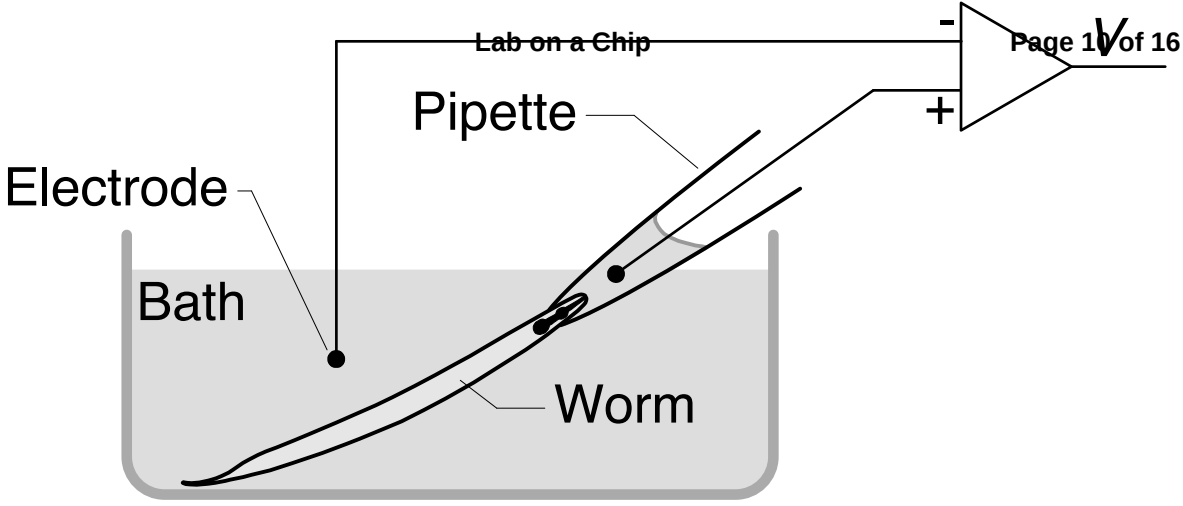
-
+
V
Pipette
Electrode
Bath
Worm

A

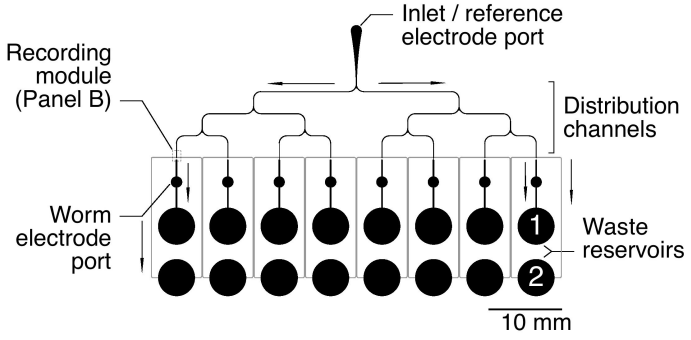
Inlet / reference
electrode port
Recording
module
(Panel B)
Distribution
channels
Worm
electrode
port
1
2
Waste
reservoirs
10 mm

B

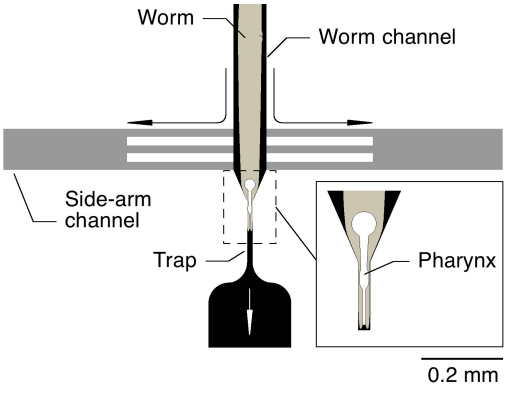
Worm
Worm channel
Side-arm
channel
Trap
Pharynx
0.2 mm

C

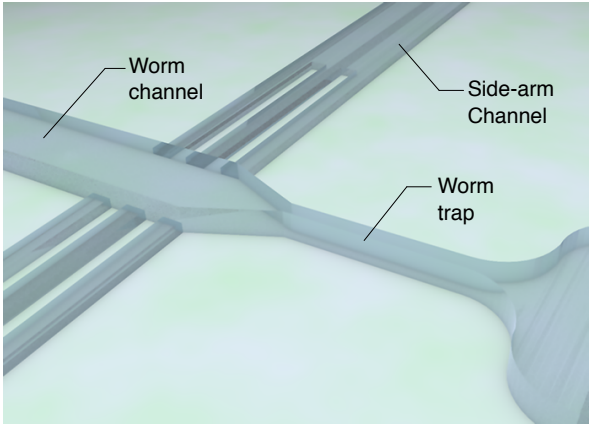
Worm
channel
Side-arm
Channel
Worm
trap

D


80 µm

E

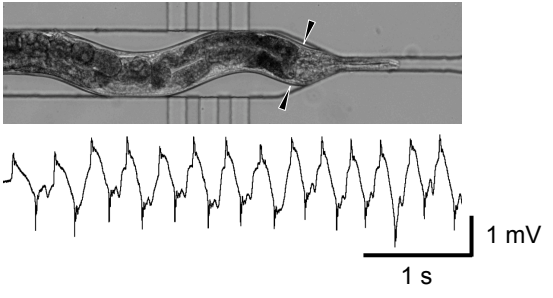
1 mV
1 s

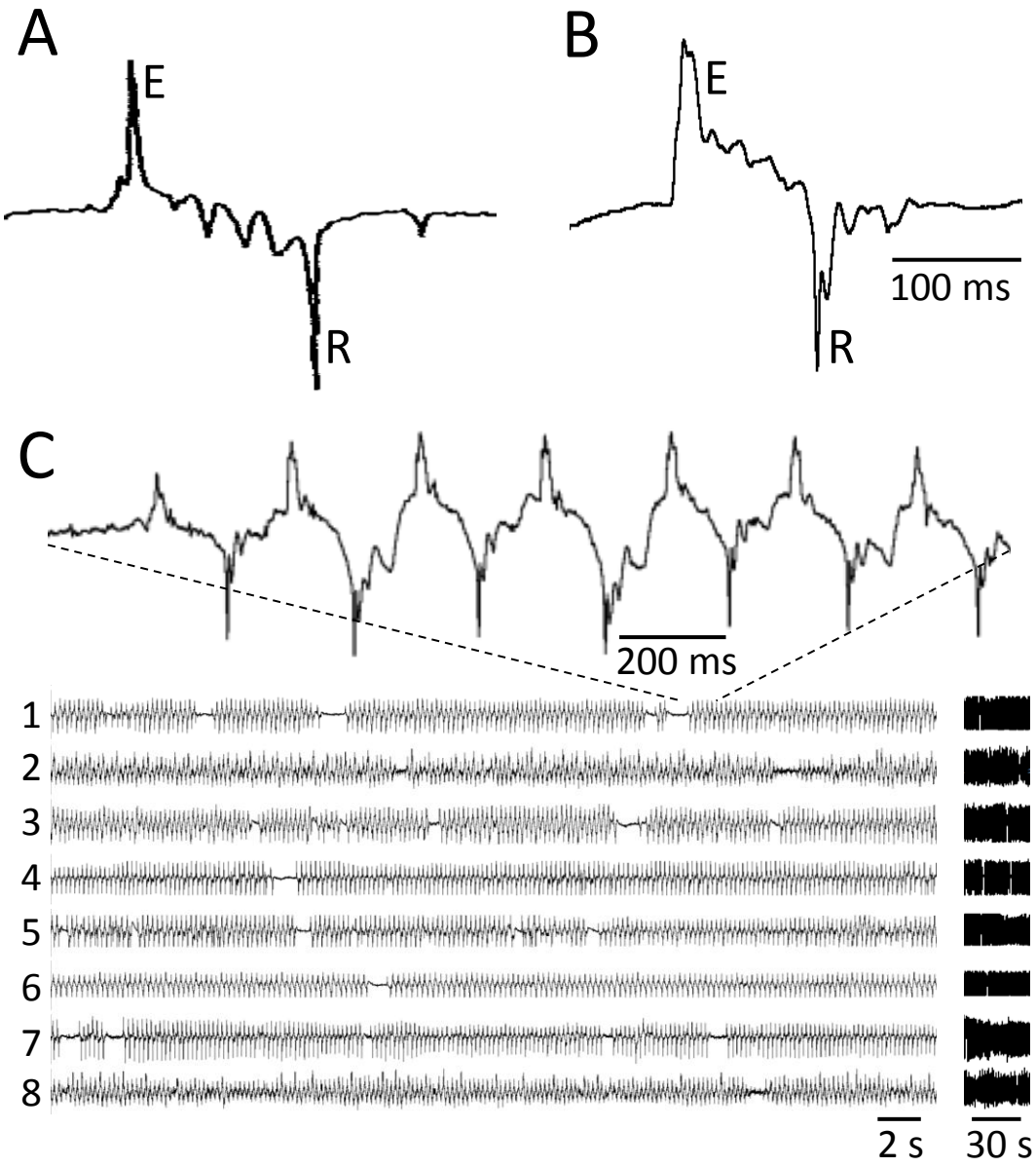
A
E
R
B
E
R
100 ms
C
200 ms
1
2
3
4
5
6
7
8
2 s
30 s

A Wild type: Control → 3 µM IVM

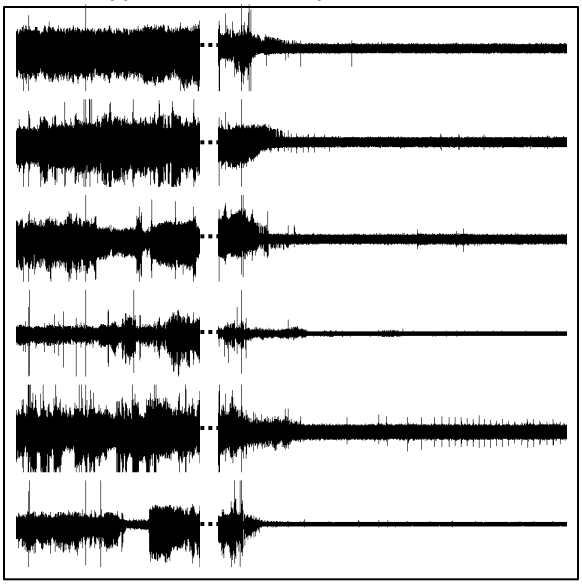

B Wild type: Control → Control

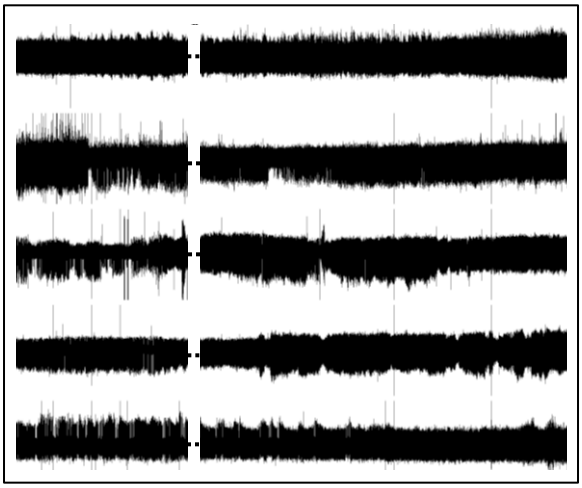

C IVM-resistant: Control → 3 µM IVM

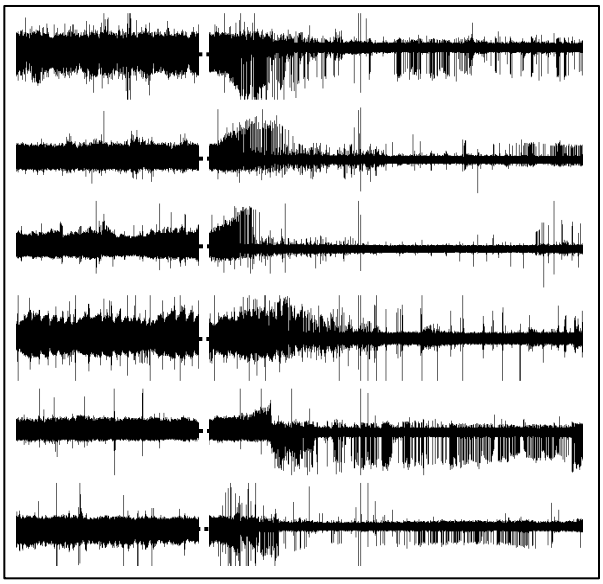

10 min

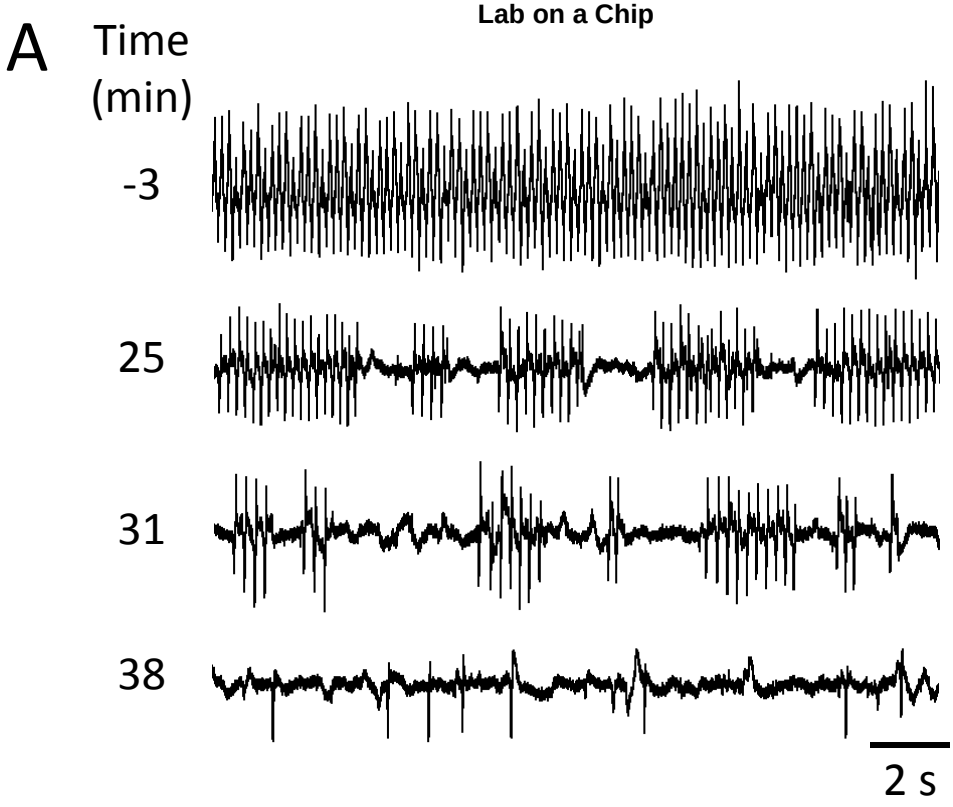
A
Time
(min)
-3
25
31
38
2 s

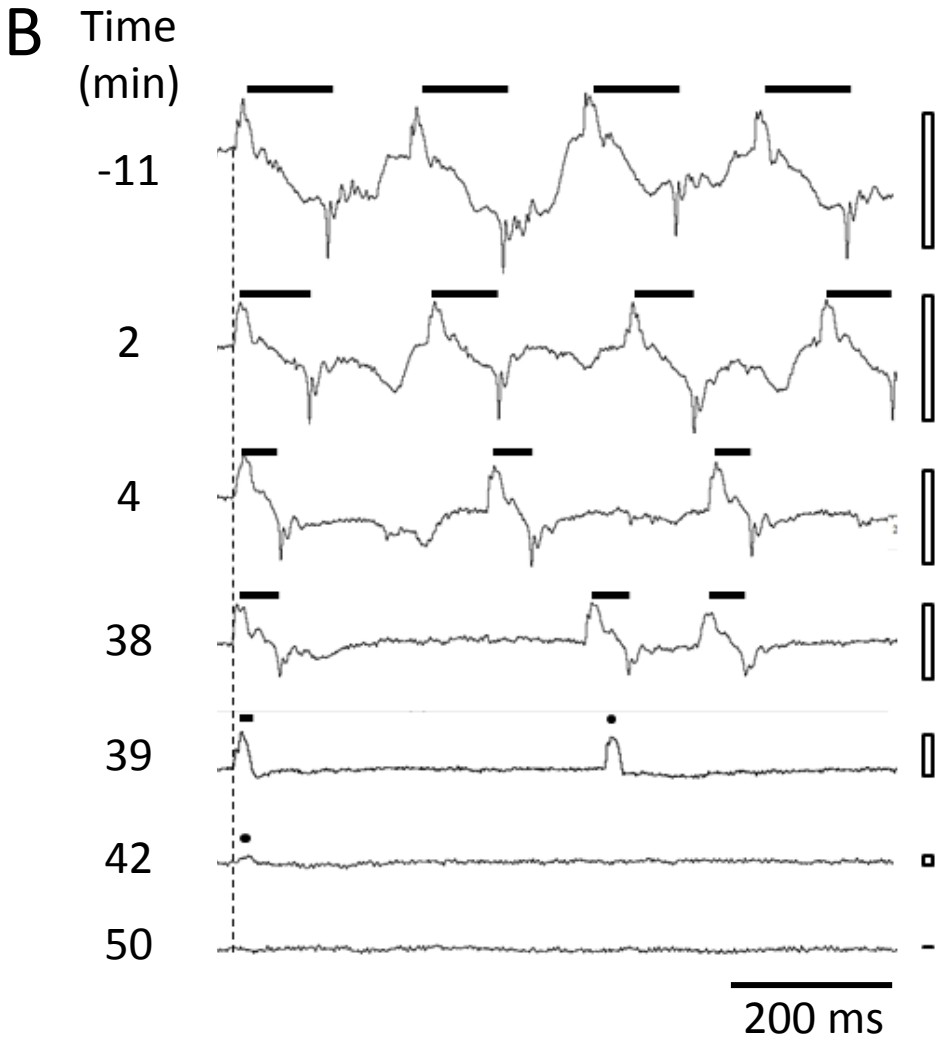
B
Time
(min)
-11
2
4
38
39
42
50
200 ms

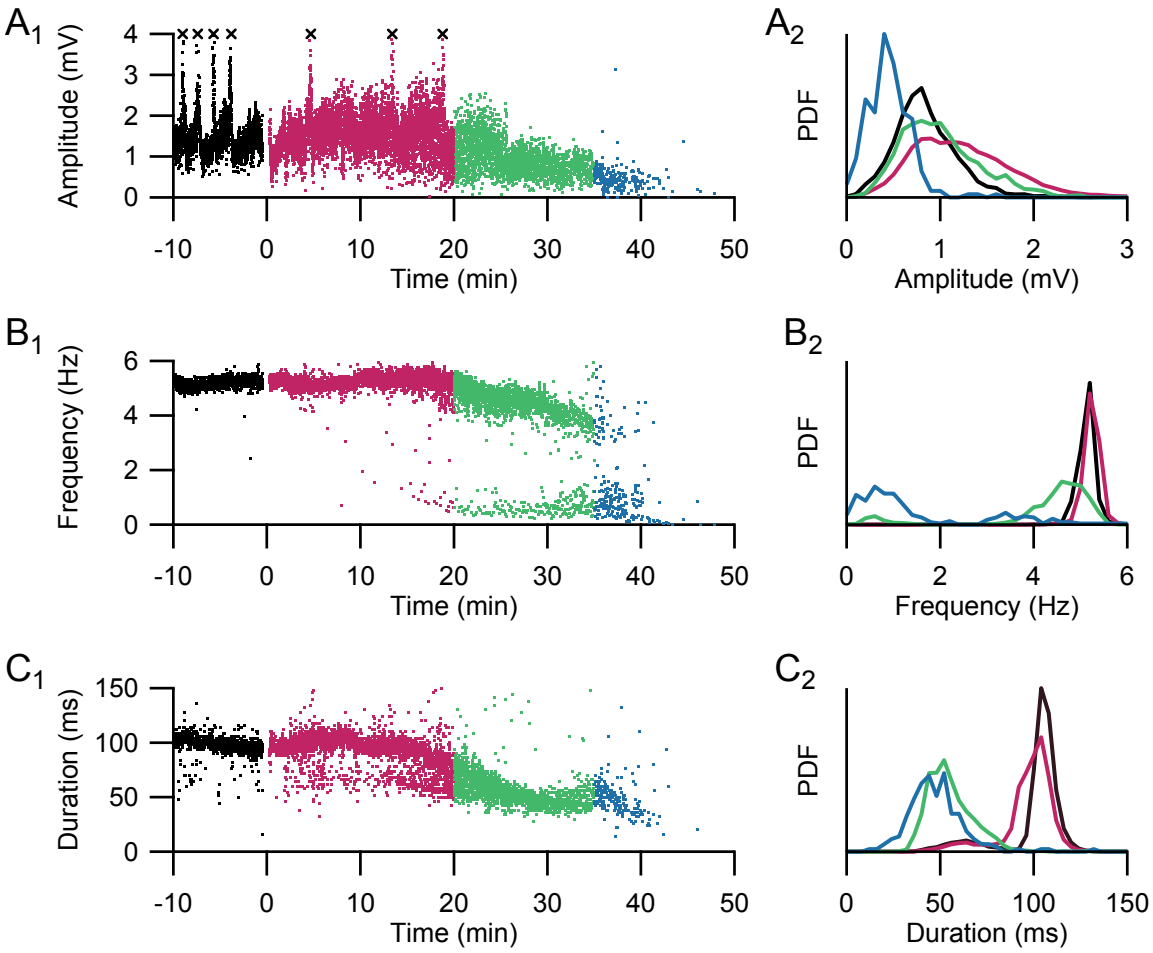
A1
Amplitude (mV)
Time (min)
A2
PDF
Amplitude (mV)
B1
Frequency (Hz)
Time (min)
B2
PDF
Frequency (Hz)
C1
Duration (ms)
Time (min)
C2
PDF
Duration (ms)

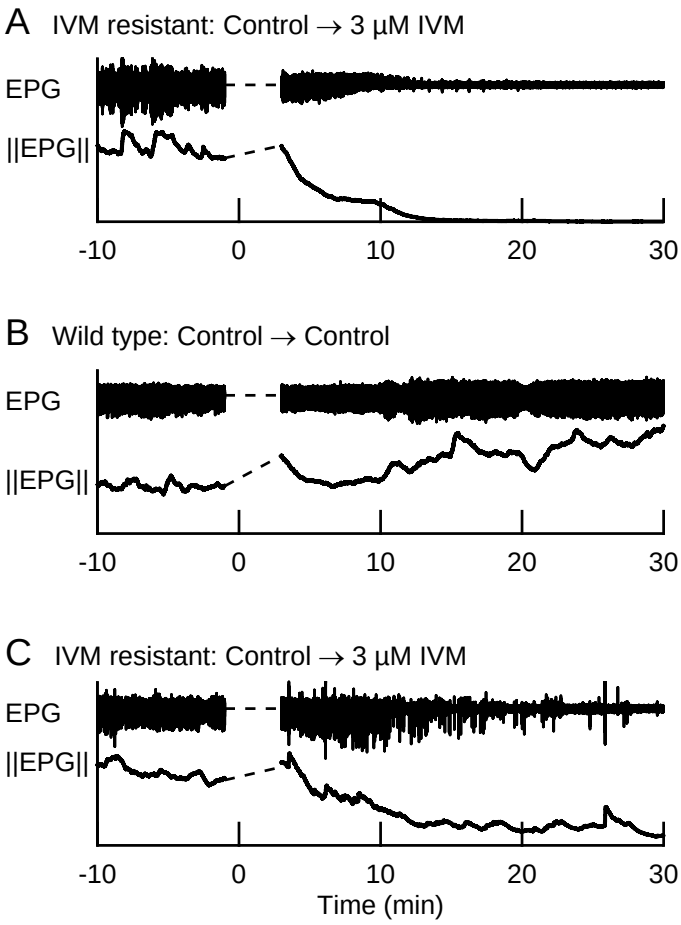
A IVM resistant: Control → 3 µM IVM
EPG
||EPG||
-10
0
10
20
30
B Wild type: Control → Control
EPG
||EPG||
-10
0
10
20
30
C IVM resistant: Control → 3 µM IVM
EPG
||EPG||
-10
0
10
20
30
Time (min)

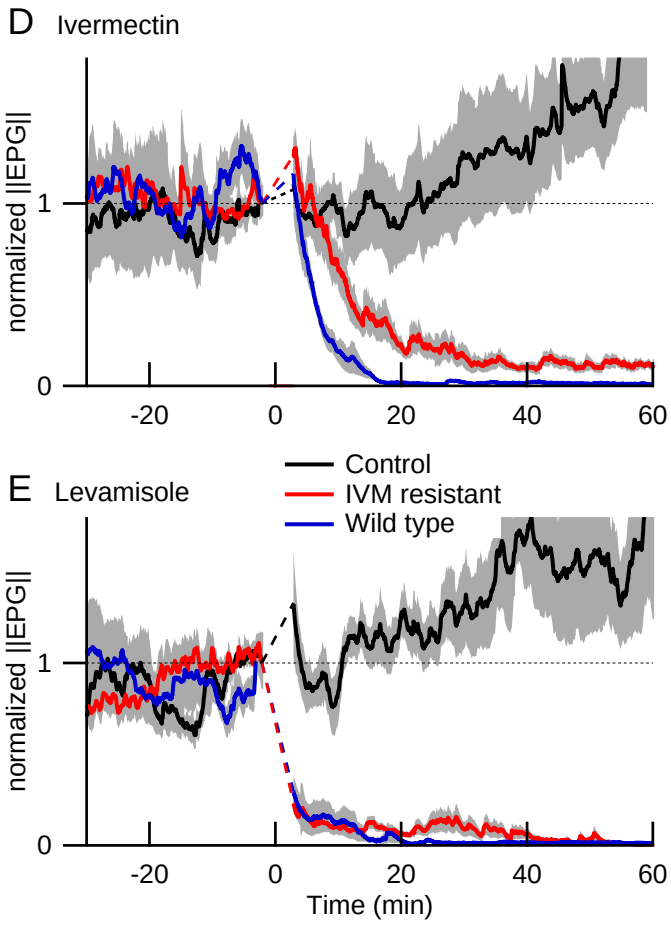
D Ivermectin
normalized ||EPG||
1
0
-20
0
20
40
60
E Levamisole
Control
IVM resistant
Wild type
normalized ||EPG||
1
0
-20
0
20
40
60
Time (min)